Relaxation Time, Activation Energy, and Reaction Pathway Determination of the Poly(ethylene glycol dimethacrylate)–Dopant (I_2) Interaction with the Nuclear Magnetic Resonance Technique

Ulku S. Ramelow, Samantha N. Braganza, Gerald J. Ramelow, Ron W. Darbeau

Department of Chemistry, McNeese State University, Lake Charles, Louisiana 70609

Received 4 May 2005; accepted 11 October 2005
DOI 10.1002/app.23854
Published online in Wiley InterScience (www.interscience.wiley.com).

ABSTRACT: Conductive polymers were obtained with a new polymerization method in which UV light was used as a photochemical initiator. In a previous work, optimum irradiation times were determined to obtain high conversion percentages. The effect of dopants on the conductivity of the polymer poly(ethylene glycol dimethacrylate) (PEGDM) was studied with $LiClO_4$ and I_2 as a dopant. The most effective dopant concentration was determined by the measurement of conductivities. Through the tracing of the conductivity change at various temperatures during the reaction of PEGDM with the dopant, the activation energies of the interactions were calculated, and a method was developed to follow the kinetics of the polymerization reaction with a conductometric technique. This work presents a nuclear magnetic resonance (NMR) study of the same polymer prepared under the optimum conditions with the results obtained in a previous study. NMR spectroscopy was used to determine the relaxation time, rate constants, and activation energy of the polymer–dopant interactions. As a preliminary study, pyruvic acid was used, and for acid-catalyzed pyruvic acid/water reactions, the relaxation time, activation energy, and enthalpy change values (ΔH) were determined. With the same NMR technique, the reaction mechanisms of the polymerization, relaxation times, and rate constants of the polymer–dopant interactions were determined. The polymerization pathway was determined with NMR spectra; the results were confirmed by the calculation of the activation energies and bond-breaking energies.
 J Appl Polym Sci 100: 5087–5101, 2006

Key words: irradiation; NMR; conducting polymer; dopant

INTRODUCTION

The development of conducting polymers can be traced to the mid-1970s.[1,2] A major discovery was that certain polymers such as polysulfonitride[3] and polyacetylene[4] can be made highly conductive in the presence of certain additives called dopants.[5]

Although the mechanism of conduction remains incompletely understood, it is believed that certain structural features influence the level of conductivity; they include delocalization (charge may be transferred through pendent groups), doping (by additional groups rearranging double bonds into a conjugated mode[6]), and morphology (conjugational and conformational factors[7,8]).

Conductive polymer resin demand in the United States is expected to increase from 270 million pounds in 1996 to 470 million pounds in 2006. This number will be nearly 600 million pounds, including additives, in 2006.[9] Improved resin grades will result in more intensive use in electronics, appliances, and electrostatic spray painting of automotive and industrial parts. Conductive polymers will control the high levels of static electricity developed by moving parts as well as electromagnetic interference (EMI)/radiofrequency interference (RFI) emissions, and they will be more effective in protecting sensitive electronic devices from static discharge during production, transportation, and storage. Recently conjugated polymers are used in biomedical applications in tissue engineering.[9]

Carbon black powders are used with conductive polymers for electrostatic discharge protection. Metallic and carbon fibers are used as additives in conductive polymers for EMI and RFI shielding.[9] There is much interest in conductive polymers because of their applications in rechargeable batteries,[10] electronic devices,[11] gas-separation membranes,[12] and enzyme immobilization[13,14] due to their electrical properties. Their practical use and processibility can be improved by the development of their poor mechanical and physical properties with chemical electrochemical blending.[15–17] In addition, their conductivity can be improved by the addition of dopants.[18,19] Solvents used during the polymerization process also have importance in increasing the conductivity of the polymer.[20]

Correspondence to: U. S. Ramelow (uramelow@mcneese.edu).

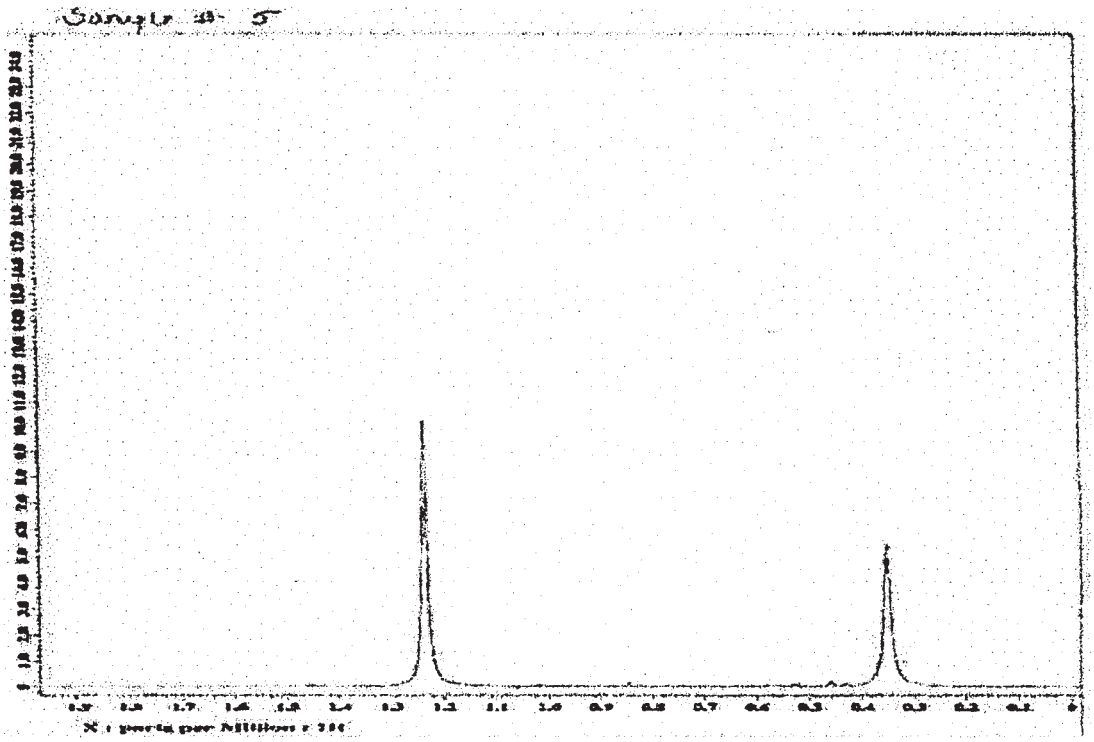

Figure 1 NMR spectrum of a system (0.50 mL of pyruvic acid + 0.35 mL of H_2O + 0.25 mL of HCl) at room temperature.

The purpose of a previous study was to obtain a new conductive polymer, poly(ethylene glycol dimethacrylate) (PEGDM), with photochemical methods (UV irradiation) to obtain high conversion percentages, to determine the optimum irradiation time, and to study the temperature effect on the conductivity of the obtained polymer.[21] Further aims were to increase the conductivity of the polymer, to incorpo-

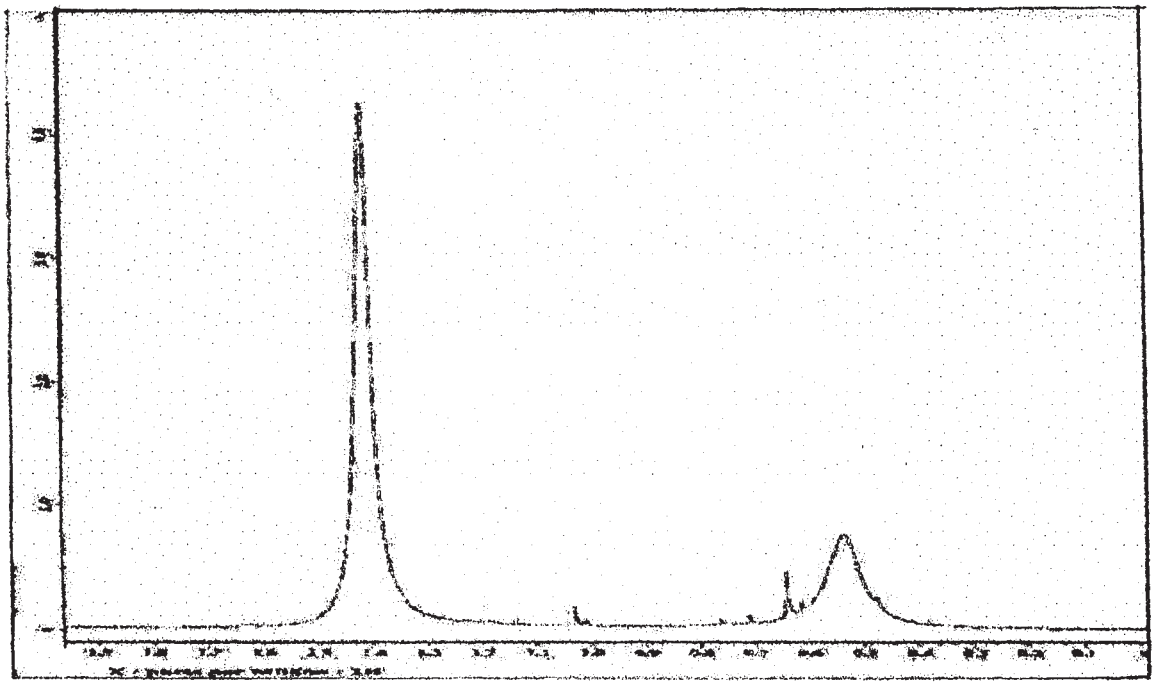

Figure 2 NMR spectrum of a system (0.50 mL of pyruvic acid + 0.35 mL of H_2O + 0.25 mL of HCl) at 40°C..

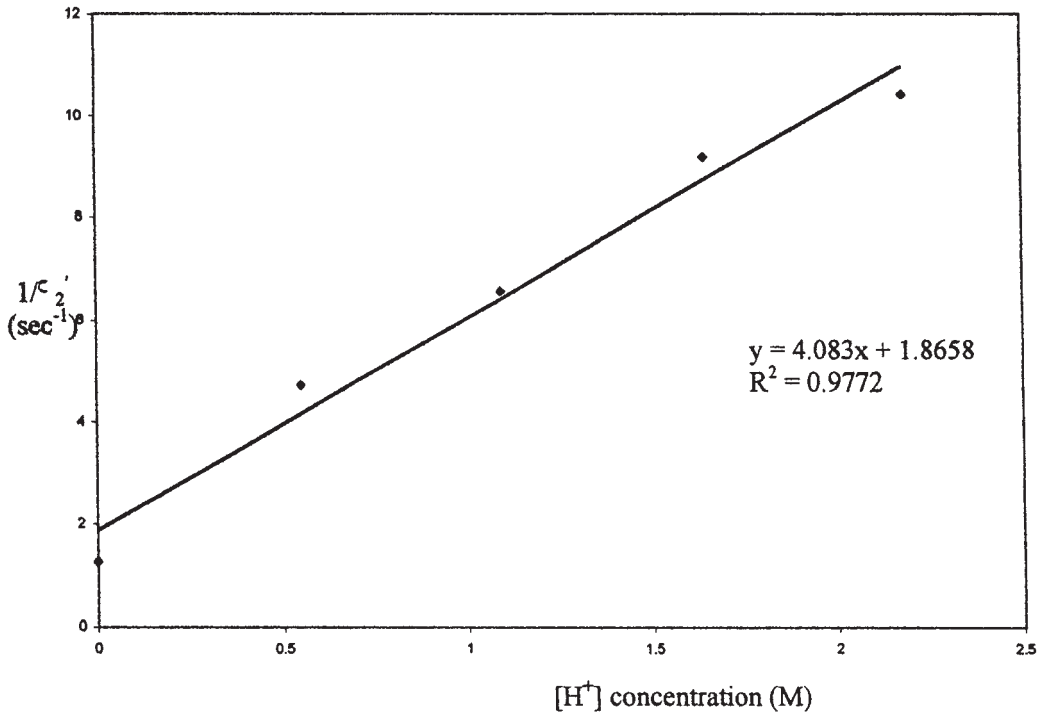

Figure 3 Plot of $1/T_2'$ versus $[H^+]$ at 1.75 ppm (at 40°C).

rate the polymer with some dopant substance such as iodine and lithium perchlorate, and to find the most effective concentrations for each dopant by tracing the conductivity while changing the dopant concentration.[21]

In this study, dopant-incorporated polymers (PEGDM) were prepared with the same methods described in a previous study.[21] The reaction mechanism of polymerization was studied with a nuclear magnetic resonance (NMR) technique. By the determination of the full width of the broadened bands at half of the band height (fwhm) to be *a* for the corresponding NMR peaks, the relaxation times and rate constants of the polymer–dopant interactions were calculated. A determination of the rate constants at different temperatures provided an estimate of the activation energies.

The calculation of the activation energy by a relaxation time technique could also provide additional information on the reaction mechanism, showing where exactly the free-radical mechanism was initiated during the polymerization process. By taking NMR spectra of polymeric samples and dopant-added samples, we could determine the mechanism of the polymerization and reaction kinetics of the dopant-incorporated polymers.

EXPERIMENTAL

Materials

Ethylene glycol dimethacrylate (EGDM) monomer was obtained from Sigma Aldrich Chemical Co. (Milwaukee, WI). It was purified of the inhibitor by vac-

TABLE I
Reaction Kinetics of Acid-Catalyzed Pyruvic Acid Reactions at Room Temperature

Solution number	Width (cm) at half-height		ζ_1' (s) at	ζ_2'' (s) at	$1/\zeta_2'$ (s^{-1})			k_{H+} (slope)	
	2.6 ppm	1.75 ppm	2.6 ppm	1.75 ppm	2.6 ppm	1.75 ppm	$[H^+]$ (*M*)	2.6 ppm	1.75 ppm
1	0.2	0.3	1.59	1.06	0.63	0.94	0		
2	0.5	0.5	0.64	0.64	1.56	1.56	0.55		
3	0.5	0.6	0.64	0.53	1.56	1.89	1.09	0.30	0.814
4	0.6	0.8	0.53	0.39	1.89	2.56	1.64		
5	0.7	0.9	0.45	0.35	2.22	2.86	2.18		
6	1.0	1.0	0.32	0.32	3.14	3.14	2.73		

TABLE II
Temperature Dependence of Acid-Catalyzed Pyruvic Reactions (at 40°C)

Solution number	Width (cm) at half-height		ζ_1' (s) at	ζ_2' (s) at	$1/\zeta_1'$ (s^{-1}) at	$1/\zeta_2'$ (s^{-1}) at		k_{H+} (slope)	
	2.6 ppm	1.75 ppm	2.6 ppm	1.75 ppm	2.6 ppm	1.75 ppm	$[H^+]$ (*M*)	2.6 ppm	1.75 ppm
1	0.3	0.4	1.06	0.79	0.94	1.26	0		
2	1.2	1.5	0.265	0.212	3.77	4.72	0.55		
3	1.3	2.1	0.245	0.152	4.08	6.58	1.09	0.43	4.083
4	1.35	2.9	0.236	0.109	4.24	9.17	1.64		
5	1.4	3.3	0.227	0.0096	4.4	10.42	2.18		
6	1.15	2.6	0.277	0.122	3.61	8.196	2.73		

uum distillation at 60–80°C at 30 mmHg. 2.2′-Azobisisobutyronitrile (AIBN) initiator was obtained from Polysciences, Inc. (Warrington, PA). It was purified of methanol before use as follows. A solution was prepared in methanol and cooled. The crystals were collected on a fritted glass filter and dried *in vacuo* at room temperature. Iodine was obtained from Mallinckrodt Chemical Works (Phillipsburg, NJ). It was used as a solid directly in a tetrahydrofuran (THF) (Aldrich) solution during the polymerization of EGDM.

Pyruvic acid, used for preliminary NMR studies, was obtained from Sigma Aldrich Chemical. It was purified by vacuum distillation at room temperature at 30 mmHg. Deuterated acetonitrile (CD_3CN) and deuterated water (D_2O) (both from Aldrich) were used as internal reference solutions for NMR studies. For UV irradiation, a Phillips HPR 125-W mercury vapor lamp was used with a maximum wavelength of 254 nm. NMR spectra were recorded on a 300-mHz FT-NMR spectrometer. All samples were degassed and irradiated in quartz tubes 12 cm high and 2.8 cm in diameter. A high-vacuum system was used (10^{-4} to 10^{-5} mmHg) for evacuating monomer solutions.

Preparation of the polymers

About 5 mL of distilled monomer EGDM, 10 mL of THF, and 1.0% inhibitor (AIBN) were placed in quartz tubes. The tubes were sealed with a septum and connected to a high-vacuum system with a syringe needle and degassed to 10^{-4} to 10^{-5} mmHg for 5–6 h. The degassed tubes were irradiated in a horizontal position at a distance of 20 cm from the UV source. After irradiation for the required time of polymerization, the obtained polymer was dissolved in THF, which was a good solvent for both the monomer and polymer, and precipitated in methanol. The obtained polymer was then filtered and dried in a vacuum oven at room temperature to a constant weight. When dopant addition was required, about 0.347*M* dopant was incorporated with the monomer solution system before

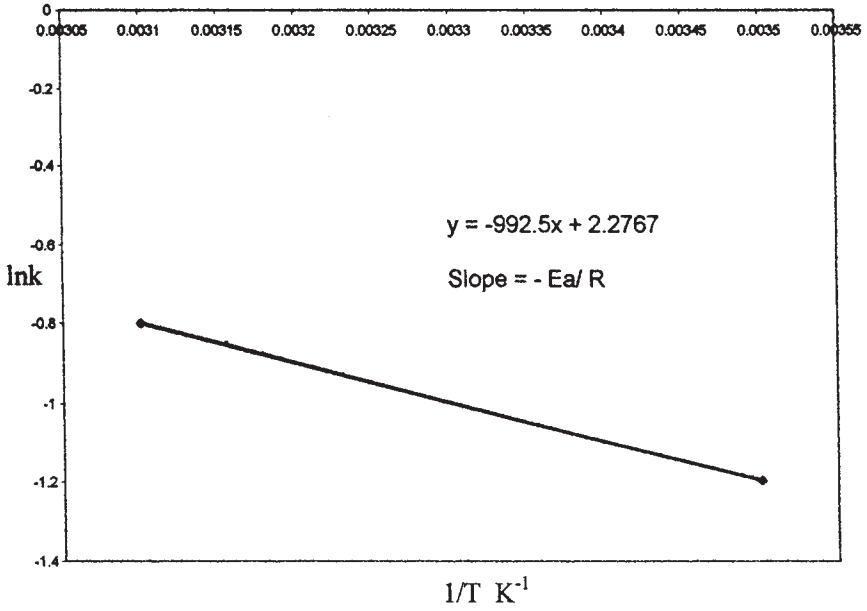

Figure 4 Plot of ln *k* versus $1/T$ for the peak at 2.6 ppm (forward reaction).

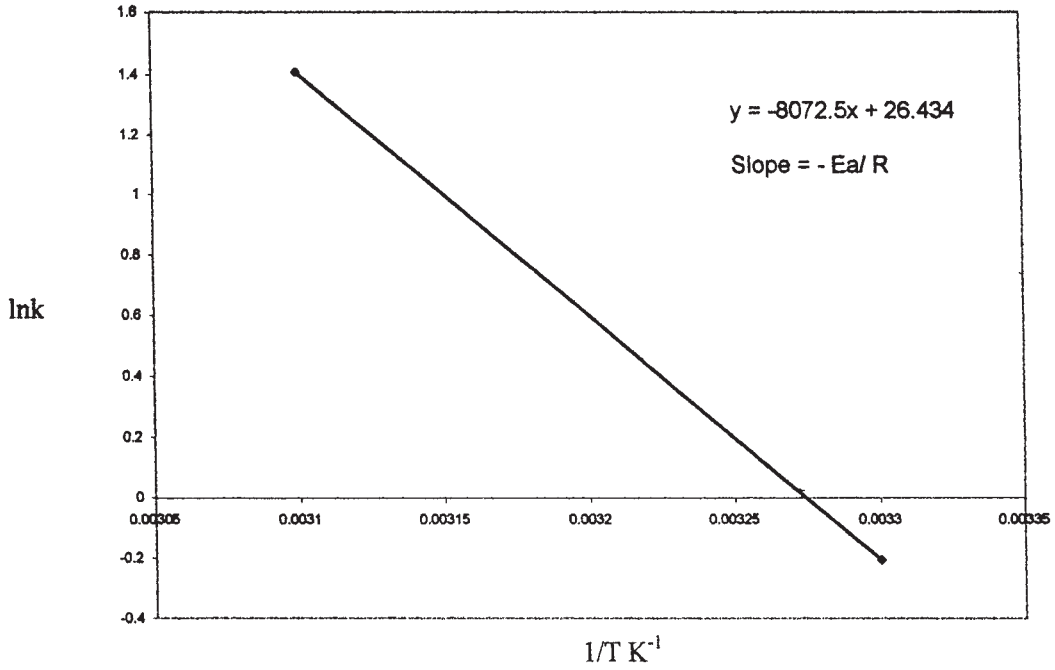

Figure 5 Plot of ln k versus $1/T$ for the peak at 1.75 ppm (reverse reaction).

polymerization, or it was added to the polymer solution after polymerization.

This work presents an NMR study for the determination of the relaxation time, activation energy, and enthalpy change (ΔH) of the polymer–dopant interaction. As a preliminary work, pyruvic acid was used for acid-catalyzed pyruvic acid reactions. With NMR spectra, the polymerization pathway was determined; it was confirmed by the calculated activation energy values.

THEORY

NMR spectroscopy provides a method for determining the reaction kinetics and pathway for polymer–dopant systems. The NMR technique is used to determine the reaction mechanism of polymerization. The relaxation times and then rate constant of the polymer–dopant interactions can be calculated by the determination of fwhm = a for the corresponding NMR peaks

Determining rate constants at different temperatures can provide an estimate of activation energies. Calculating activation energies by a relaxation time technique can also provide additional information about the reaction mechanism, showing where exactly the free-radical mechanism is initiated during the polymerization process. By taking NMR spectra of polymeric samples and dopant-added systems, we can determine the mechanism of the polymerization and the reaction kinetics of the dopant-incorporated polymers.

The fwhm is inversely proportional to the net relaxation time (T_2') for the proton:

$$\mathrm{F}(a)(\mathrm{Hz}) = 1/\pi \times T_2' \tag{1}$$

$$1/T_2' = 1/T_2 + 1/\zeta \tag{2}$$

where T_2' is related to the relaxation time of the fully exchanged protons, T_2 is the relaxation time in the absence of the exchange, and ζ is the lifetime. The rate of the acid-added reaction is proportional to the acid concentration. Thus, eq. (2) can be written in the form of eq. (3):

$$1/T_2' = \mathrm{Constant} + k[\mathrm{H}^+] \tag{3}$$

A plot of $1/T_2'$ versus the H^+ concentration should yield a straight line with a slope equal to the value for the dopant-added rate constant, k. By measuring the fwhm of mean peak resonances in NMR spectra, we can calculate the relaxation times and rate constants. The Arrhenius theory of the reaction rates predicts the temperature dependence of the rate constants:

$$k = Ae^{-E^a/RT} \tag{4}$$

where E_a is the activation energy of the reaction, A is a unit-bearing pre-exponential factor, R is the gas constant, and T is the temperature. Equation (4) leads to the so-called Arrhenius plot:

$$\ln k = \ln A - \frac{E_a}{RT} \tag{5}$$

Thus, a plot of ln k versus the reciprocal of the temperature should yield a straight line, and the activation energy can be calculated from the slope.

For an acid-catalyzed reaction such as acid-catalyzed pyruvic acid, rate constants can be calculated for the peaks corresponding to the forward and reverse reactions at two different temperatures with the relaxation time method. The activation energies for these two peaks can be calculated for both forward reactions ($E_{a(f)}$) and reverse reactions ($E_{a(r)}$) from the slope of ln k–$1/T$ plots. Because in the activation energy diagram the difference between $E_{a(f)}$ and $E_{a(r)}$ is equal to the internal energy change (ΔU), this value becomes equal to ΔU and consequently because of the following equation given

$$\Delta U = \Delta H + P\Delta V \tag{6}$$

becomes equal to ΔH at a constant pressure; since there is no volume change (ΔV), volume change value is 0.

At the same time, the equilibrium constant (K_{eq}) is equal to the ratio of the rate constants:

$$K_{eq} = k_{forward}/k_{reverse} \tag{7}$$

From the van't Hoff equation

$$d(\ln K_p)/dT = \Delta H^o/RT^2 \tag{8}$$

the relation between two K_{eq} values at two different temperatures can be written as follows:

$$\ln[K_{eq(1)}/K_{eq(2)}] = -\Delta H^o/R(1/T_1 - 1/T_2) \tag{9}$$

K_{eq} values can be calculated for two different temperatures, and with eq. (9), the standard enthalpy change (ΔH^0) value can be calculated, which should yield the same result as that calculated with activation energies with eq. (5).

RESULTS AND DISCUSSION

NMR study of pyruvic acid

For the preliminary work, we decided to use pyruvic acid to see if the NMR technique was applicable to the determination of the reaction rate constants.[22–26] After pyruvic acid was purified, six different concentrations of pyruvic acid solutions were prepared:[22–26]

1. 0.50 mL of pyruvic acid and 0.60 mL of water.
2. 0.50 mL of pyruvic acid, 0.55 mL of water, and 0.05 mL of HCl.
3. 0.50 mL of pyruvic acid, 0.50 mL of water, and 0.10 mL of HCl.
4. 0.50 mL of pyruvic acid, 0.45 mL of water, and 0.15 mL of HCl.
5. 0.50 mL of pyruvic acid, 0.40 mL of water, and 0.20 mL of HCl.
6. 0.50 mL of pyruvic acid, 0.35 mL of water, and 0.25 mL of HCl.

The spectrum of pyruvic acid systems were then recorded with D_2O as the internal reference solution. Figures 1 and 2 show the NMR spectra of one of these six samples taken at room temperature and 40°C, respectively. Each spectrum for all six samples was then expanded to show only the methyl peaks at 1.75 and 2.6 ppm. The results were recorded for all six solutions with the same scale after the expansion of the two acid methyl resonances and the calculation of their widths at half-height.

The reaction between pyruvic acid and water follows both uncatalyzed and acid-catalyzed pathways, as shown in eq. (10):[22–26]

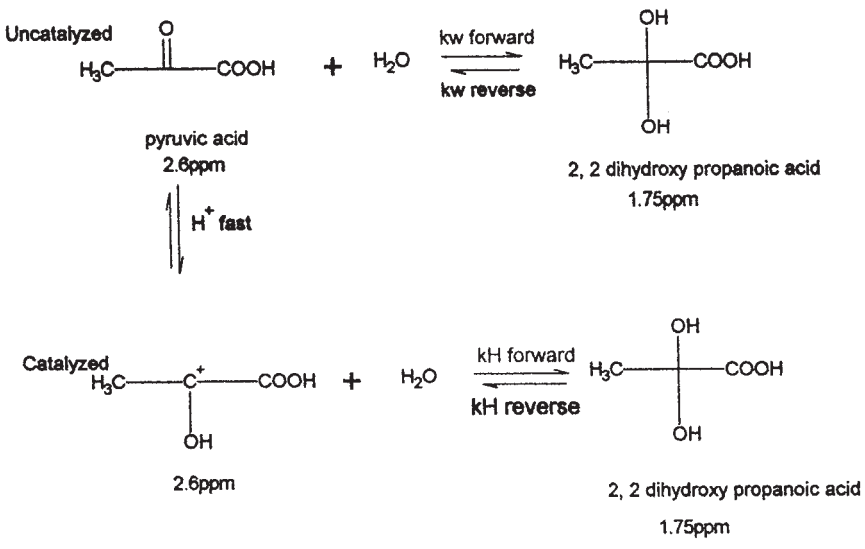

TABLE III
Reaction Rate Constant and E_a Determination of Uncatalyzed and Catalyzed Reactions Between Pyruvic Acid and Water

Temperature (K)	k		ln k		$1/T$ (K^{-1})	K_{eq} ($k_{2.6}/k_{1.75}$)	E_a (kJ/mol)	
	2.6 ppm	1.75 ppm	2.6 ppm	1.75 ppm			2.6 ppm	1.75 ppm
298	0.302	0.814	−1.197	−0.2055	0.0035	0.3709	8.251	67.114
313	0.43	4.083	−0.8	1.409	0.0031	0.1053		
ΔH^* (kJ/mol) by $E_{af} - E_{ar}$				ln K_{eq}			ΔH^* (kJ/mol) by eq. (9)	
−58.86				−0.992 −2.631			−65.1	

The bands at 2.6 and 1.75 ppm represent the resonances of the methyl protons of pyruvic acid and 2,2-dihydroxy proprionic acid, respectively. fwhm is inversely proportional to T_2' for the proton, as given in eq. (1). T_2' is also related to ζ according to eq. (2).

The rate of the acid-catalyzed reaction is proportional to the concentration of the protonated pyruvic acid, which in turn is proportional to the H^+ concentration. Thus, the acid-catalyzed rate is $k_H = [H^+]$ and can be written as given in eq. (3). A plot of $1/T_2'$ versus the H^+ concentration should yield a straight line with a slope equal to the acid-catalyzed rate constant k_{H+}.

For two different temperatures (room temperature and 40°C), the rate constants for the forward (at 2.6 ppm) and reverse (1.75 ppm) reactions were calculated from the slopes of $1/T_2'$ versus H^+. Figure 3 shows one of the plots for the results at 40°C. The results are given in Tables I and II.

The Arrhenius theory of reaction rates predicts the temperature dependence of the rate constants, as given in eq. (4). This equation leads to eq. (5). Thus, a plot of ln k versus the reciprocal of the absolute temperature results in a straight line; from the slope, the activation energy can be determined. Figures 4 and 5

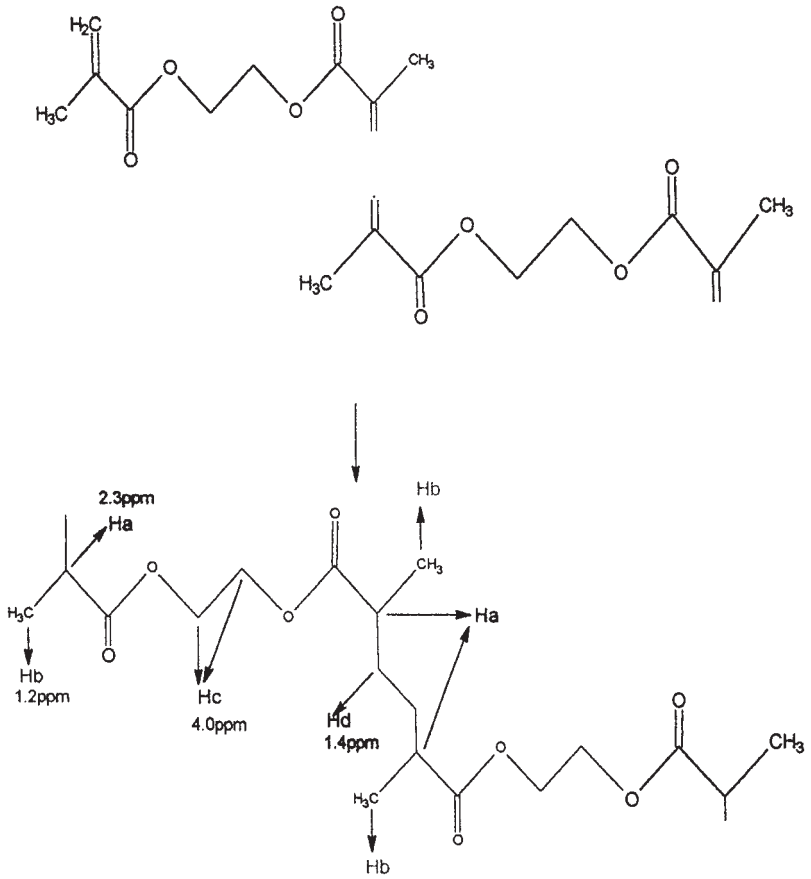

Figure 6 Suggested polymerization pathway of EGDM.

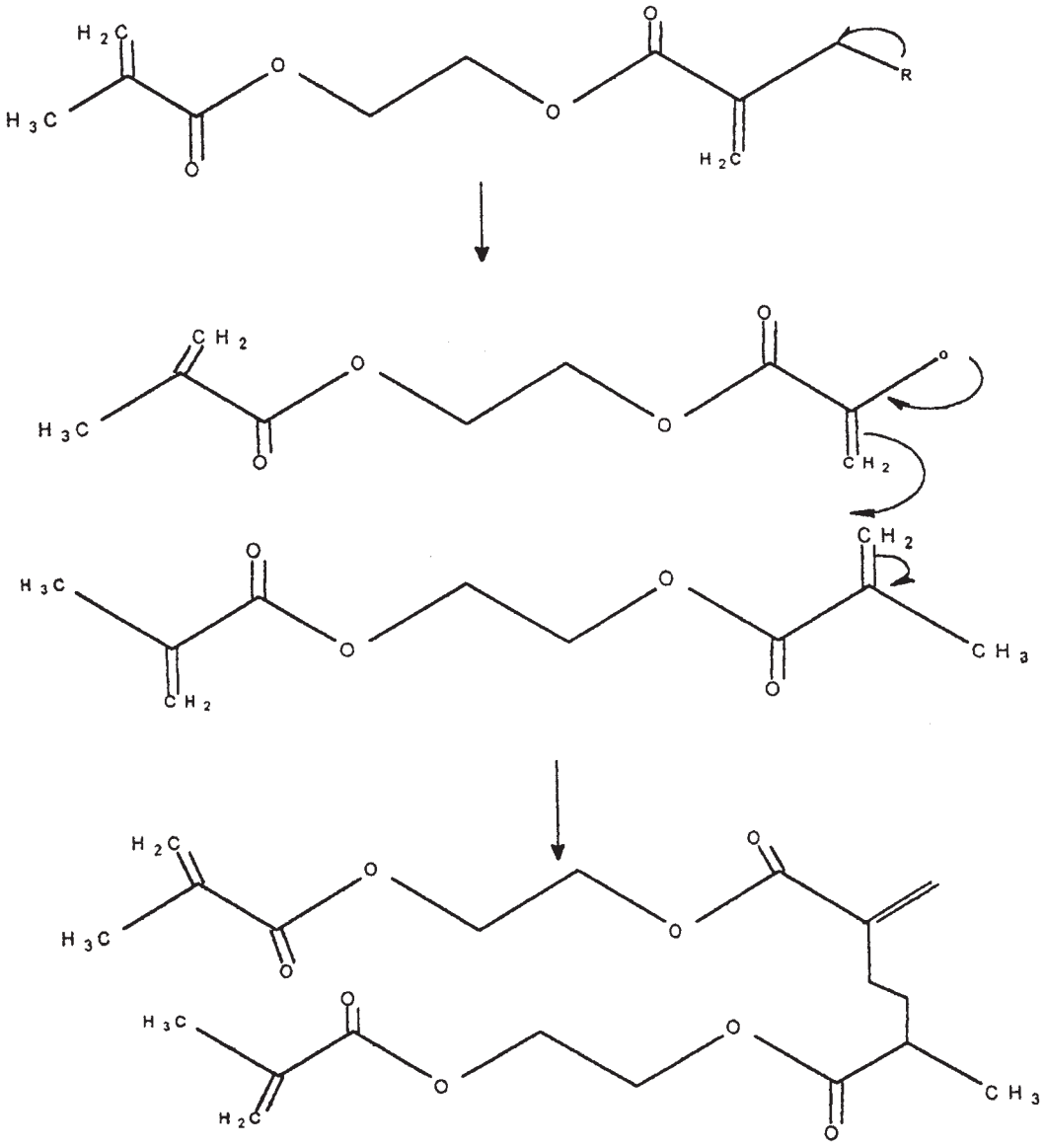

Figure 7 Path A: breaking across the C—CH_3 bond.

show such plots for 2.6 and 1.75 ppm peaks, corresponding to the forward and reverse reactions. From the slopes of these plots, activation energies were calculated for the forward and reverse reactions. Because each point in this plot was calculated with six different samples for each temperature, they are considered very solid points; thus, taking only two points for two different temperatures was sufficient. The results are summarized in Table III. In an activation energy diagram (potential energy vs reaction coordinate), the difference between $E_{a(f)}$ and $E_{a(r)}$ is equal to ΔU. The ΔU value calculated in this manner turns out to be equal to −58.86 kJ/mol. This value is also equal to ΔH of the reaction at a constant pressure according to eq. (6).

At the same time, K_{eq} is equal to the ratio of rate constants, as given in eq. (7), where $k_{forward}$ and $k_{reverse}$ values correspond to the peaks at 2.6 and 1.75 ppm, respectively. K_{eq} values were calculated for two different temperatures, and with eq. (9), ΔH^0 was calculated to be −65.1 kJ/mol. This value is very close to the enthalpy value calculated with activation energies. Therefore, it is concluded that NMR provides a convenient technique for studying reaction kinetics, and it was decided to use the same technique for the study of dopant-added polymerization. The results are presented in Table III.

NMR study of PEGDM

Dopant added before polymerization

For the NMR study, the sample tubes were prepared with the following procedure. Iodine was added to the

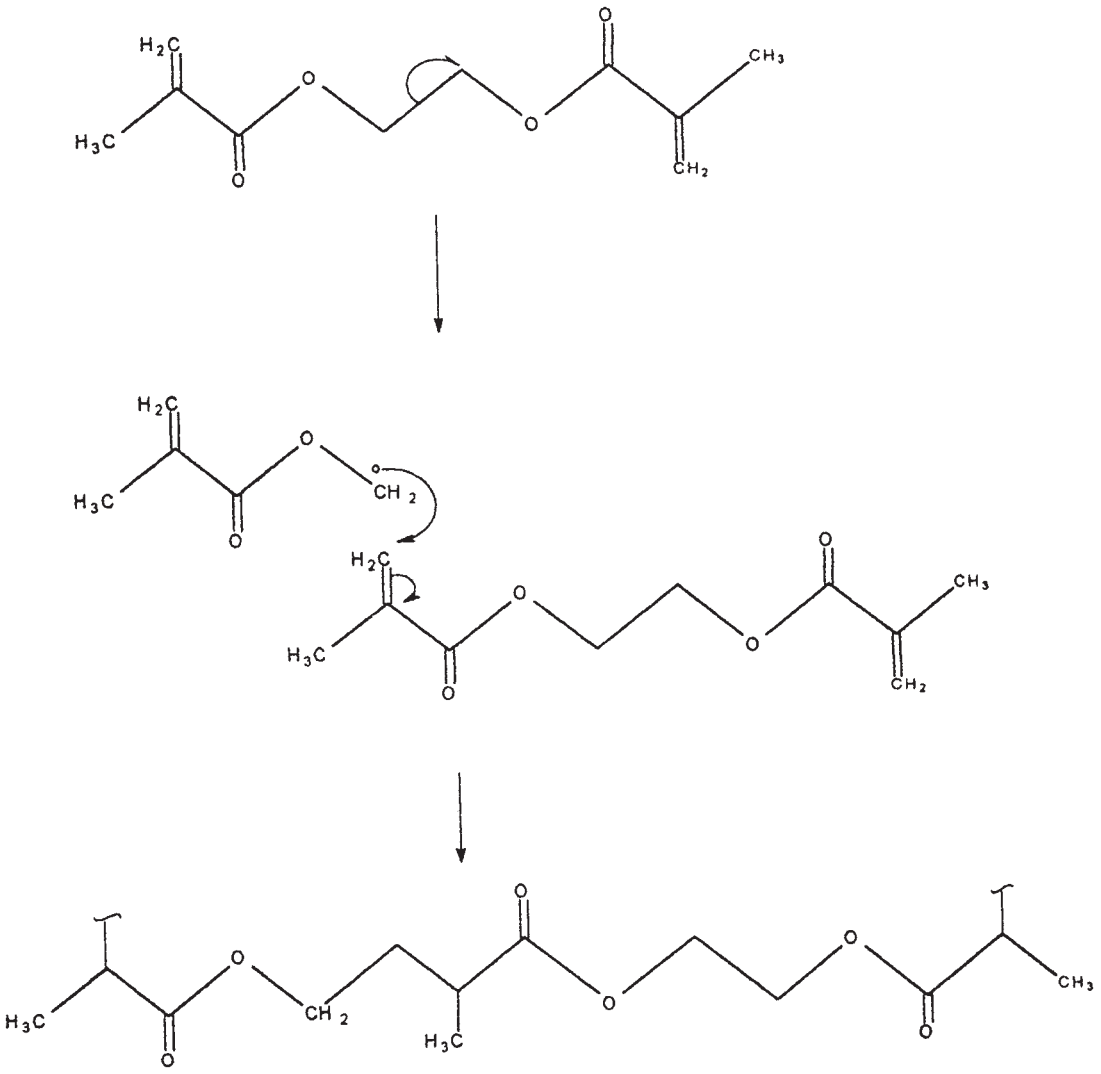

Figure 8 Path B: breaking across the H_2C—CH_2 bond.

monomer mixture (5.0 mL of EGDM + 10.0 mL of THF + 1% AIBN + 0.5*M* I_2) before irradiation. However, there was no polymer obtained when I_2 was introduced before UV irradiation. This is attributed to the following mechanism: although the monomer radical is formed by UV irradiation, at the same time, I_2 with UV light forms iodine radicals, which cause termination in the polymerization reaction. The reactions can be summarized as follow:

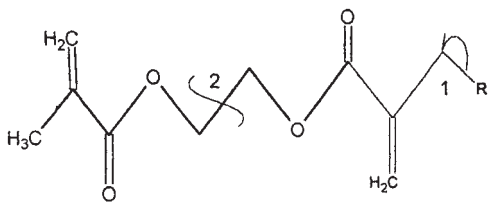

Figure 9 Two possible pathways for free-radical polymerization.

$$M \xrightarrow{h\nu} M\cdot \quad I_2 \xrightarrow{h\nu} 2I\cdot \quad M\cdot + I\cdot \rightarrow MI \tag{11}$$

As a result, no polymer was obtained.

Dopant added after polymerization

The most effective dopant concentration with I_2 as a dopant was calculated by a conductivity method from plots of the conductivity versus the I_2 concentration,[21] and it was found to be 0.5*M*. The most effective irradiation time was also determined by the measurement of the conductivities of iodine-incorporated PEGDM samples with iodine from plots of the conductivity versus the irradiation time.[21] The maximum conductivity was achieved after 3.0 h of irradiation. The conductivity of polymers obtained after 3.0 h of irradiation without any dopant was 1.24 μs; when iodine was

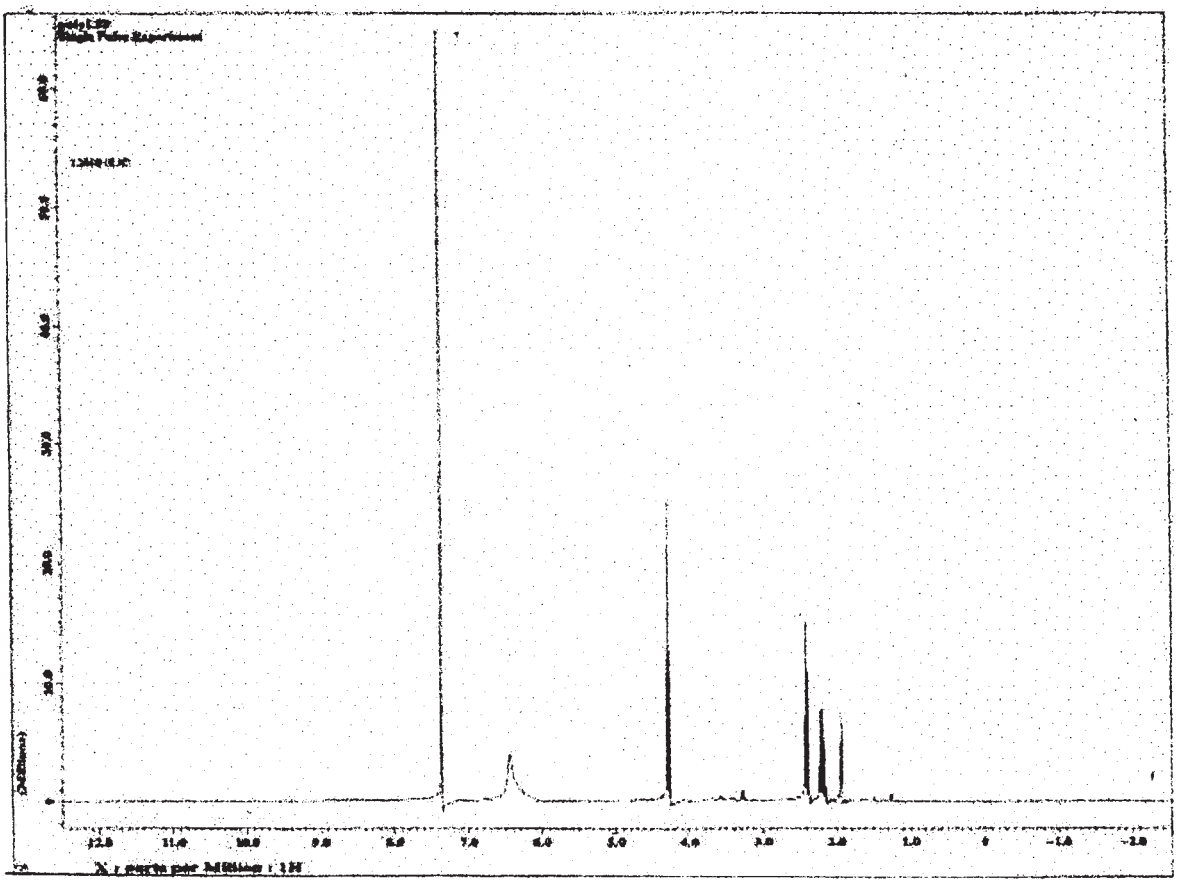

Figure 10 NMR spectrum of PEGDM incorporated with I_2 (after 3 h of UV irradiation) at room temperature (25.3°C; 0.125 g of PEGDM + 12.5 mL of THF + 1.2*M* I_2).

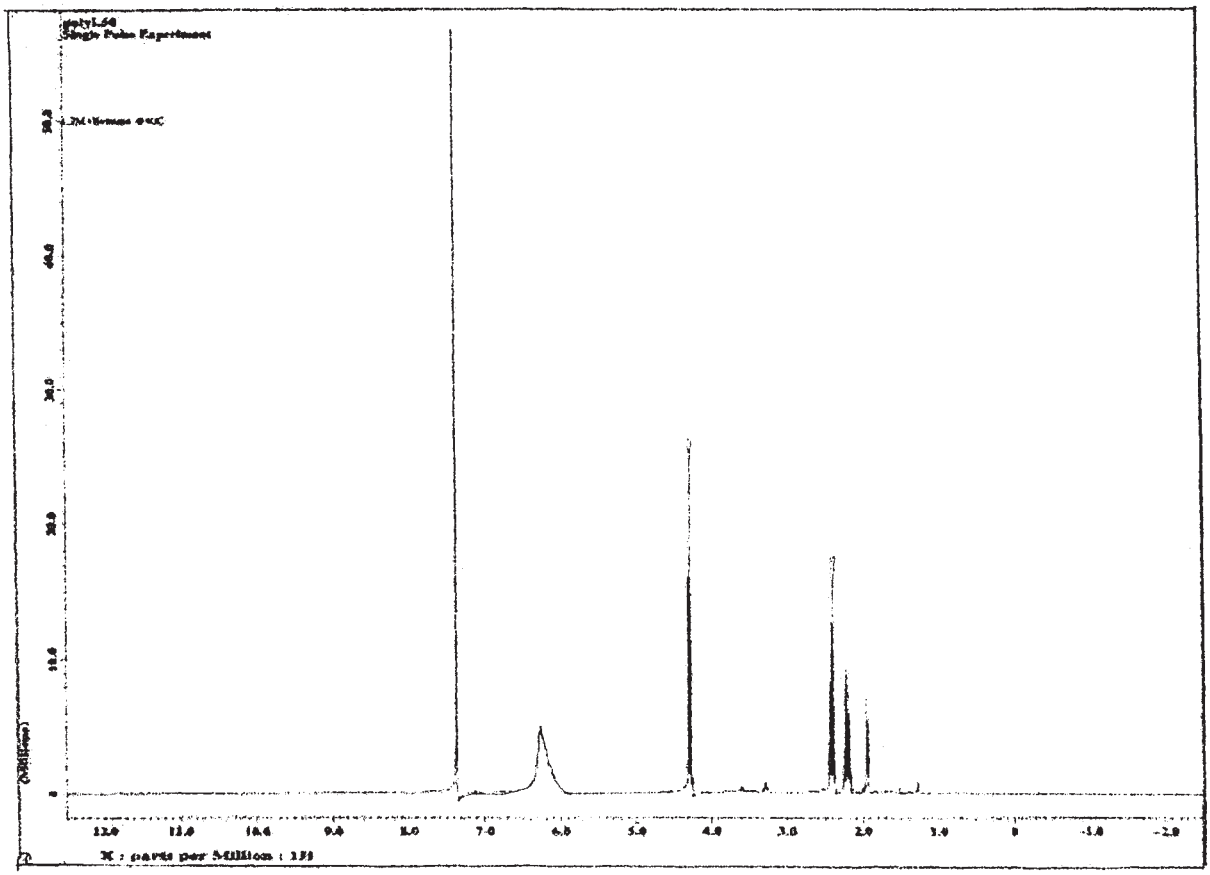

Figure 11 NMR spectrum of PEGDM incorporated with I_2 (after 3 h of UV irradiation) at 40°C (0.125 g of PEGDM + 12.5 mL of THF + 1.2*M* I_2).

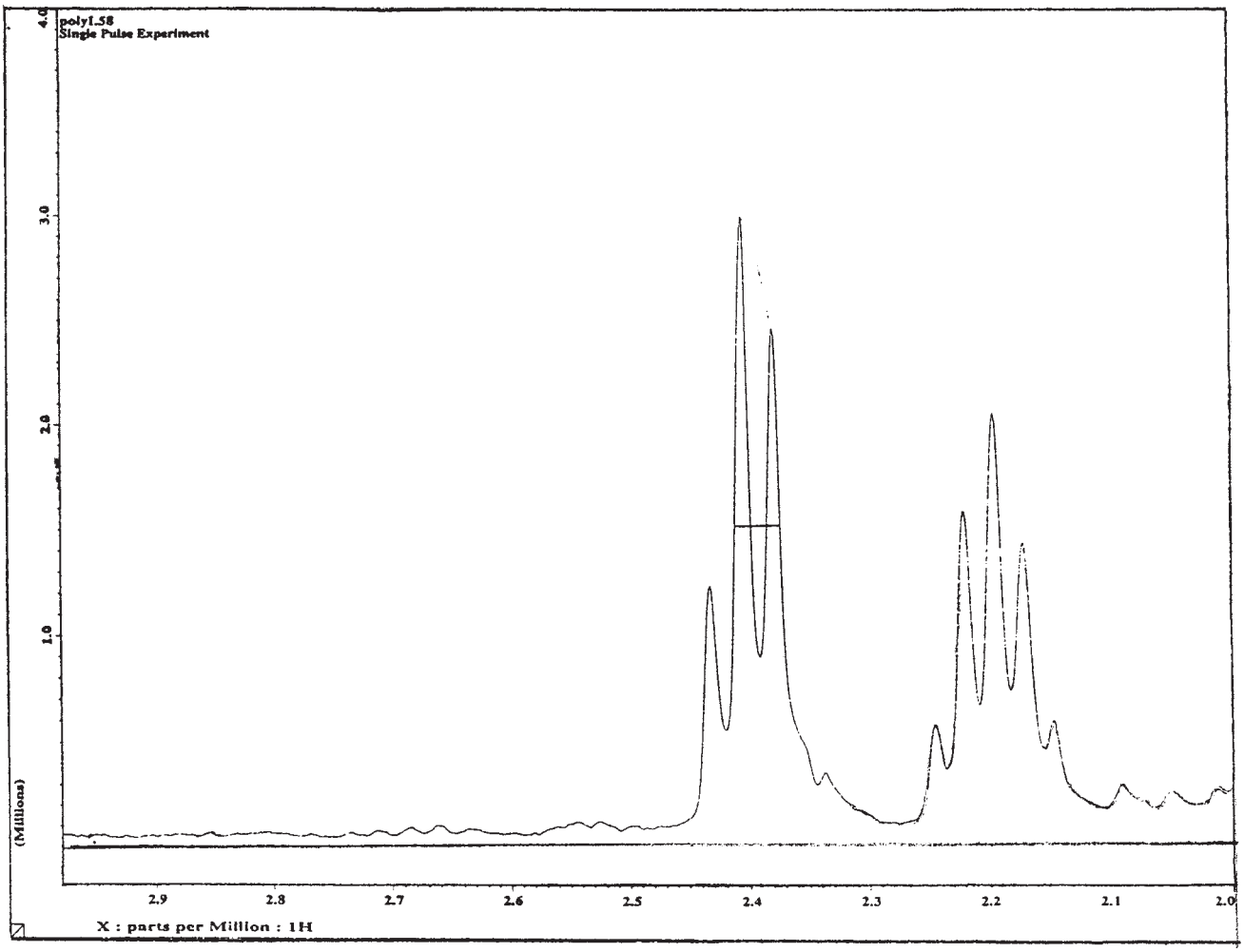

Figure 12 Expanded NMR spectrum of 2.4 ppm showing the full width at half-height of the —CH_3 peak.

added after 3.0 h of irradiation, the conductivity increased to 60.8 μs. This indicates that iodine increases the conductivity value by about 60 times. However, this study is focused only on the kinetics of polymer–dopant interactions with an NMR technique.

In a typical run, 50 mg of the obtained polymer sample that was incorporated with iodine was put into an NMR tube, and 750 μL of the solvent (acetonitrile-d_3) was added. The sample was then loaded into the NMR probe at room temperature and later at 40°C. ^{1}H-NMR spectra were taken for different samples of the polymer prepared with various concentrations of iodine.

The maximum observed variation in the probe temperature during runs was 0.2°C. The signals observed for the polymer PEGDM show the following peaks (^{1}H-NMR, CD_3CN): 4.3 (t), 2.4 (d, 2H), 2.3 (m), and 1.4 (d, 2H). The suggested polymerization is given in Figure 6 with the corresponding ppm values. This figure presents the suggested polymerization pathway of EGDM, by which polymerization would normally take place across the double bond. However, this was not observed when the ^{1}H-NMR spectrum of PEGDM was taken. Evidence showed that the signals were not corresponding and that the multiplicity did not match at all. The methylene groups (—CH_2—CH_2—), which were supposed to appear in the region of δ = 4.0 ppm with the combination of two monomers, were not observed in the NMR signal. This implies that polymerization takes place by a free-radical process. For the free-radical polymerization, possible pathways are across the C—CH_3 bond (path A) and —CH_2—CH_2— bond (path B).

Figures 7 (path A) and 8 (path B) present the mechanisms of two possible pathways by which free-radical polymerizations take place. These two pathways are both possible for the free-radical polymerization of EGDM, as summarized in Figure 9. To find out the most probable pathway, the corresponding bond-breaking energies were calculated for both —C—CH_3 and —CH_2—CH_2— bonds.

Mercury vapor UV light with a wavelength of 254 nm was used for the irradiation. The corresponding energy for the UV light was calculated with the equa-

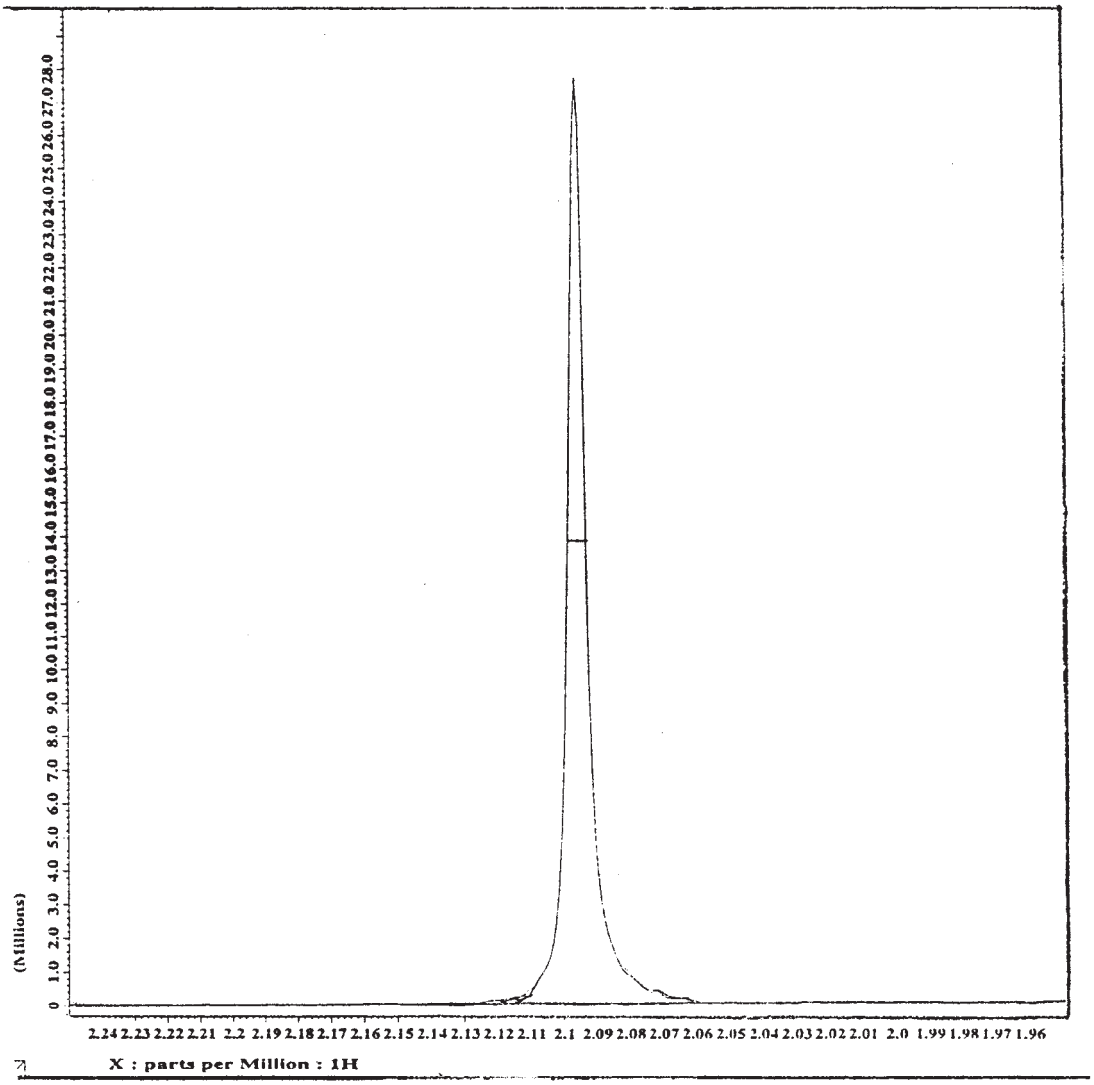

Figure 13 Expanded NMR spectrum of 4.3 ppm showing the full width at half-height of the —H_2C—CH_2 peak.

tion $\Delta E = h\nu$, where h is Planck's constant and ν is the frequency equal to c/λ. The energy of UV light was calculated to be 78×10^{-20} J/photon. Because by UV irradiation one photon can activate only one molecule, the energy can be represented as 78×10^{-20} J/molecule. The energy required to break the C—CH_3 bond was determined to be 61.2×10^{-20} J/molecule (with the binding energy for C—CH_3 to be 88 kcal/mol).[27] In a similar manner, the energy required to break the CH_2—CH_2 bond was calculated to be 57.8×10^{-20} J/molecule by assuming the binding energy for the C—C bond to be 348 kJ/mol.[28] In the presence of oxygen atoms (—O—CH_2—CH_2—O—) in the molecular structure, this would be much smaller because

TABLE IV
Reaction Kinetics of Polymer–I_2 Interactions at Room Temperature (25.3°C)

Solution number	Width (cm) at half-height		ζ_1' (s) at	ζ_2' (s) at	$1/\zeta_1'$ (s^{-1}) at	$1/\zeta_2'$ (s^{-1}) at		k_1 (slope) at	k_2 (slope) at
	4.3 ppm	2.4 ppm	4.3 ppm	2.4 ppm	4.3 ppm	2.4 ppm	I_2 (M)	4.3 ppm	2.4 ppm
1	1.4	1.5	2.243	2.093	0.446	0.477	0.2		
2	1.7	1.6	1.847	1.9625	0.541	0.5095	0.5		
3	1.5	1.8	2.093	1.744	0.477	0.573	0.8	0.32	0.16
4	1.6	1.6	1.9625	1.9625	0.5095	0.5095	1		
5	1.8	1.5	1.744	2.093	0.573	0.477	1.2		

TABLE V
Temperature Dependence of Polymer–I_2 Interactions at 40°C

Solution number	Width (cm) at half-height		ζ_1' (s) at	ζ_2' (s) at	$1/\zeta_1'$ (s^{-1}) at	$1/\zeta_2'$ (s^{-1}) at		k_1 (slope) at	k_2 (slope) at
	4.3 ppm	2.3 ppm	4.3 ppm	2.3 ppm	4.3 ppm	2.3 ppm	I_2 (M)	4.3 ppm	2.4 ppm
1	1.4	1.0	2.243	3.14	0.446	0.318	0.2		
2	1.2	1.0	2.616	3.14	0.382	0.318	0.5		
3	1.4	1.0	2.243	3.14	0.446	0.318	0.8	0.32	3.9
4	1.3	0.9	2.415	3.48	0.414	0.287	1		
5	1.2	0.8	2.616	3.92	0.382	0.255	1.2		

oxygen is highly electronegative and pulls the bond on either side. As a result, it has been calculated that the energy of UV light is capable of breaking both the C—CH_3 and CH_2—CH_2 bonds, but the possibility of breaking the CH_2—CH_2 bond is more probable. Thus, the polymerization of EGDM can be considered to follow both pathways A and B; however, because the energy required to break the CH_2—CH_2 bond is smaller, free-radical polymerization most likely follows pathway B.

Relaxation time and activation energy determination of the dopant (I_2)–polymer interaction

First, the relaxation time of interaction was determined by the same method applied to pyruvic acid. Six different NMR samples were prepared by the placement of 50 mg of the obtained polymer samples incorporated with different concentrations of iodine. For each run, 750 μL of the solvent (acetonitrile-d_3) was added to the polymer, and ^{1}H-NMR spectrum was taken immediately at room temperature (25.3°C) for each sample prepared with a different dopant concentration. Figures 10 and 11 show two NMR spectra for one of the polymer–I_2 systems (0.125 g of polymer + 12.5 mL of THF + 1.2M I_2) at two different temperatures (25.3 and 40°C). The spectra of the I_2-doped polymer samples consist of two bands. The bands at 2.4 and 4.3 ppm represent the resonances of —CH_3 and —CH_2—CH_2— protons, respectively. Each spectrum was expanded to show —CH_3 and —CH_2—CH_2— peaks at 2.4 and 4.3 ppm. Figures 12

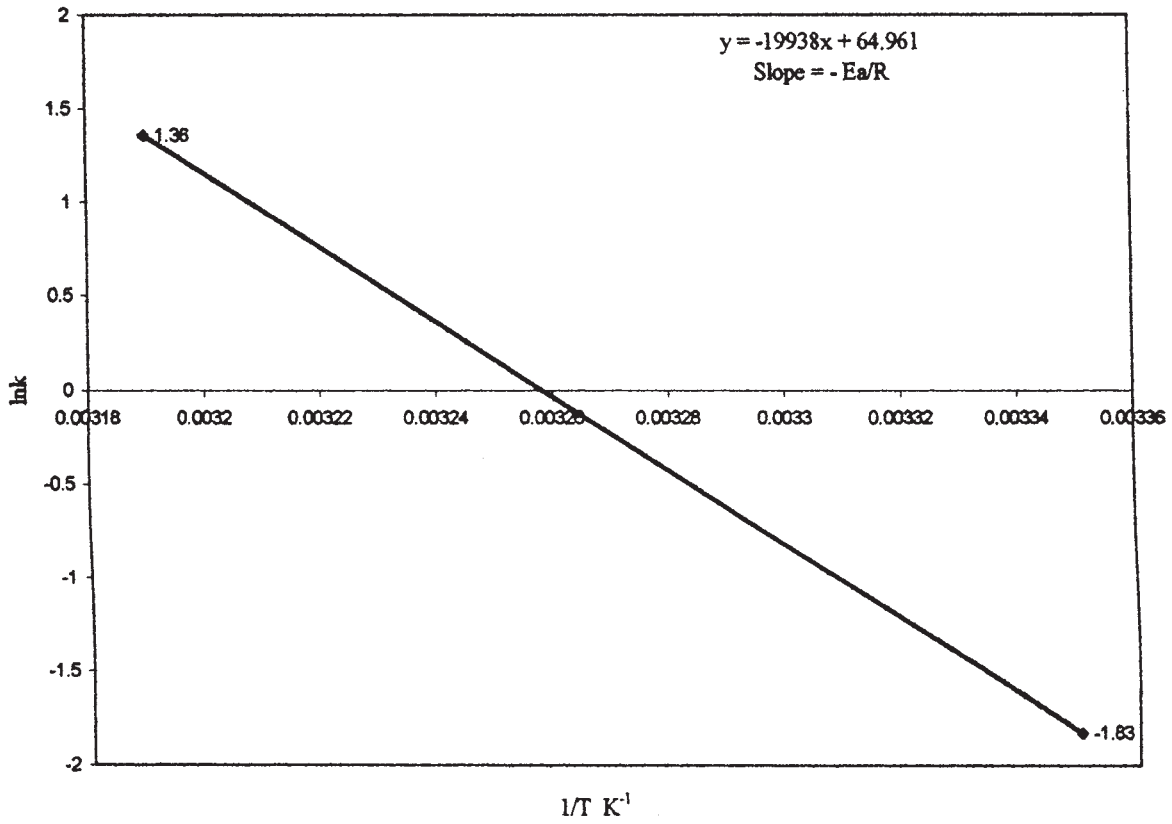

Figure 14 Plot of ln k versus $1/T$ at 2.4 ppm.

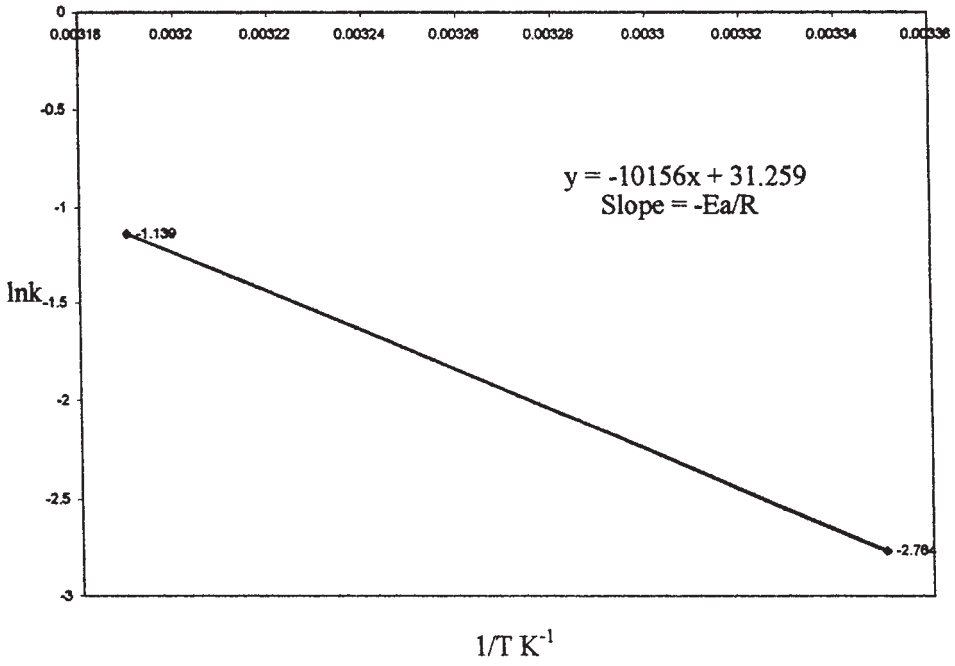

Figure 15 Plot of ln k versus $1/T$ at 4.3 ppm.

and 13 show expanded NMR spectra at the corresponding peaks. The peak width at half-height (fwhm = a) was calculated for each peak at two different temperatures for five different polymer–dopant samples. The fwhm = a value is related to the relaxation time in the manner shown in eq. (1). The relaxation time for each sample was calculated with that equation.

The rate constants k_1 and k_2 for 2.4 and 4.3 ppm peaks were calculated after the conversion of eq. (3) into the following form:

$$1/T_2' = \text{Constant} + k[I_2] \qquad (12)$$

This shows the relation between the rate constant and relaxation time for I_2-added polymers. The rate constants were calculated with plots of $1/T_2'$ versus I_2 concentrations. The same experiment was repeated at another temperature (40°C). Tables IV and V show the results of the reaction kinetics at 25.3 and 40°C, respectively. For each temperature, the rate constants at 2.3 and 4.3 ppm were calculated.

The activation energy of interaction for the I_2 dopant with the polymer (PEGDM) when I_2 was attacking the —CH_3 bond (2.4 ppm) and the —CH_2—CH_2— bond (4.3 ppm) was calculated after the rate constant values were obtained for these peaks at two different temperatures. A plot of ln k versus the reciprocal temperature resulted in a straight line with a negative slope of magnitude $-E_a/R$ [eq. (5)]. Figures 14 and 15 shows the plots at 2.4 and 4.3 ppm, respectively. The corresponding activation energies of interaction were calculated to be 165.764 and 64.436 kJ/mol, respectively. The results are shown in Table VI.

Because the activation energy for the 4.3 ppm interaction is much lower than the activation energy for 2.4 ppm, it provides additional evidence that the dopant attack occurs on the —CH_2—CH_2— bond rather than the —CH_3 bond. These results agree with previously obtained results in which —CH_2—CH_2— bond breaking by a free-radical polymerization process was determined to be the more probable mechanism as calculated by bond-breaking energies.

TABLE VI
Reaction Rate Constant and E_a Determination of Polymer–I_2 Interactions

Temperature (K)	k_1 at 4.3 ppm	k_2 at 2.4 ppm	ln k_1 at 4.3 ppm	ln k_2 at 2.3 ppm	$1/T$ (K^{-1})	E_a (kJ/mol)	
						4.3 ppm	2.4 ppm
296	0.32	0.16	−2.764	−1.83	0.00336	64.436	165.764
313	0.32	3.9	−1.139	1.36	0.00319		

References

1. Chiang, C. K.; Drug, M. A.; Se, G.; Heeger, A. J.; Louis, E. J.; Mac Diarmid, A. J.; Park, Y. W.; Shirakawa, H. J Am Chem Soc 1978, 100, 1013.
2. Samuelson, L. A.; Druy, M. S. Macromolecules 1986, 19, 824.
3. Moelter, G. M.; Tetrault, R. F.; Heffland, N. Polym News 1983, 9, 134.
4. Srinivas, P. R.; Mahadevan, V.; Srinivason, M. J Polym Sci Polym Chem Ed 1982, 20, 3095.
5. Handbook of Conducting Polymers; Skotheim, T. A., Ed.; Marcel Dekker: New York, 1986; Vols. 1 and 2.
6. Thakur, M. Macromolecules 1988, 21, 661.
7. Lei, J.; Cai, Z.; Martin, C. R. Synth Met 1992, 46, 53.
8. Korshak, V. V.; Vinogradova, S.; Vygodsskii, Y. S. Rev Macromol Chem 1974, 12, 45.
9. Aminabhavi, T. M.; Brannon-Peppas, L.; et al. Polym News 2002, 27, 389.
10. Peres, R. C. D.; DePaoli, M. A. J Power Sources 1992, 40, 299.
11. Diaz, A. F.; Castillo, J. I.; Logan, T. A.; Lee, W. J. J Electroanal Chem 1981, 129, 115.
12. Pellagrino, J.; Radebaugh, R.; Mattes, B. R. Macromolecules 1996, 29, 4985.
13. Selampinar, F.; Akbulut, U.; Orden, M. Y.; Toppore, L. Biomaterials 1997, 92, 1163.
14. Kizilyar, N.; Orden, N. Y.; Toppore, L.; Yager, Y. Synth Mater 1999, 104, 45.
15. Wang, H. L.; Toppore, L.; Ferandes, J. E. Macromolecules 1990, 23, 1053.
16. Yurtsever, M.; Toppore, L. Polymer 1990, 40, 5459.
17. De Paoli, M.; Panero, S.; Prosperi, P.; Scrosati, B. Electrochem Acta 1981, 129, 115.
18. Ramelow, U. S.; Ma, J.; Darbeau, R. Mater Res Innovat 2001, 5, 40.
19. Ma, J.; Ramelow, U. S.; Tauber, J. D. Tr J Chem 1997, 21, 313.
20. Ramelow, U. S.; Darbeau, R.; Ma, J.; Glenn, G.; Garrison, J. Mater Res Innovat 2004, 8, 21.
21. Ramelow, U.; Braganza, S. J Appl Polym Sci, to appear.
22. Magnetic Resonance Spectroscopy; Advanced Chemical Instrumentation Laboratory 5.33 Experiment; MIT Department of Chemistry: Cambridge, MA, 1994.
23. Brittain, E. F. H.; George, W. D.; Wells, G. H. J. Introduction to Molecular Spectroscopy, Theory and Experiment; Academic: New York, 1970.
24. Shoemaker, D. P.; Garland, C. W.; Nibler, J. W. Experiments in Physical Chemistry, 5th ed.; McGraw-Hill: New York, 1989; p 552.
25. Dyer, J. Applications of Absorption Spectroscopy of Organic Compounds; Prentice-Hall: Englewood Cliffs, NJ, 1961; p 58.
26. Pasto, D. J.; Johnson, C. R. Organic Structure Determination; Prentice-Hall: Englewood Cliffs, NJ, 1979; p 180.
27. Fesenden, R. J.; Fesenden, J. S. Organic Chemistry, 3rd ed.; Brooks/Cole: Pacific Grove, CA, 1986; p 19.
28. Atkins, P. Physical Chemistry, 6th ed.; Freeman: New York, 1998; p 941.